World Electric Vehicle Journal

MDPI

Review

A Review of Position Sensorless Compound Control for PMSM Drives

Yong Li [1,*], Han Hu [1] and Peicheng Shi [2,*]

[1] Automotive Engineering Research Institute, Jiangsu University, Zhenjiang 212013, China
[2] Automotive New Technique of Anhui Province Engineering Technology Research Center, Anhui Polytechnic University, Wuhu 241000, China
* Correspondence: liyong@ujs.edu.cn (Y.L.); shipeicheng@ahpu.edu.cn (P.S.)

Abstract: As position sensorless control technology can avoid many disadvantages caused by mechanical position sensors, improve the reliability of the motor, reduce costs and other advantages, a large number of researchers have conducted research on compound control technology in order to achieve position sensorless control technology in a wide speed range. In this article, the position sensorless compound control technology of a permanent magnet synchronous motor is reviewed, and the compound control technology of a permanent magnet synchronous motor without a position sensor is elaborated. Finally, the existing problems and development trend of sensorless compound control technology are summarized and prospected.

Keywords: permanent magnet synchronous machine (PMSM); position sensorless compound control; high frequency (HF) signal injection method; I/F control; model-based techniques

Citation: Li, Y.; Hu, H.; Shi, P. A Review of Position Sensorless Compound Control for PMSM Drives. *World Electr. Veh. J.* **2023**, *14*, 34. https://doi.org/10.3390/wevj14020034

Academic Editors: Joeri Van Mierlo and Walter Lhomme

Received: 16 December 2022
Revised: 4 January 2023
Accepted: 19 January 2023
Published: 30 January 2023

1. Introduction

In recent years, with the shortage of energy and the deterioration of the environment, energy conservation and environmental protection have become the main theme of the development of automobiles in the future [1–5]. Permanent magnet synchronous motors (PMSMs) have been continuously improved in the field of automotive motor applications due to their high-power density, large torque inertia ratio and fast dynamic response speed [6]. To achieve high performance control of the motors, the current vector and the rotor position must be synchronized. Therefore, the exact position of the rotor needs to be obtained in real time [7]. Many mechanical detection devices, such as an optical encoder and a rotary encoder, are usually installed on the motor to detect the rotor position [8]. However, the traditional motor rotor position observer occupies a certain size, which is not conducive to the installation of the motor and can also cause the motor to go out of control due to sensor faults working in harsh operating environments [9,10]. Thus, position sensorless control technology plays a key role in the field of PMSM research [11–13].

The research on position sensorless control technology for PMSM is gradually maturing and is currently focused on two main aspects of position sensorless control technology for zero- and low-speed and for medium- and high-speed operation [14,15]. As shown in Figure 1 and Table 1, the former relies on the saliency of the motor, including high-frequency (HF) signal injection [16–23], etc.; the latter generally relies on the mathematical model of the motor and is usually divided into two categories: open-loop algorithms, including direct calculation [24–27], the back electromotive force (BEMF) integration method [28–30], flux estimation [31,32], etc., and closed-loop algorithms, including the model reference adaptation system (MRAS) [33–38], sliding mode observer (SMO) [39–42], etc.

While the current position sensorless control technology at zero–low speed and medium–high speed is now well established, it is still a weak point in the full-speed domain, which appeals to numerous researchers for improvement. In the zero–low-speed range, saliency-based position sensorless control techniques are able to estimate the motor speed and position signal very well; similarly, in the medium- and high-speed range, model-based control algorithms have very good performance. As a result, most of the current position sensorless control techniques in the full-speed range are compound control technology, which combine control techniques at zero–low speed with control techniques at medium and high speed, and use switching algorithms to achieve a smooth switch between the two algorithms in the over-range. The block diagram of the compound control structure in the full-speed domain is generally shown in Figure 2.

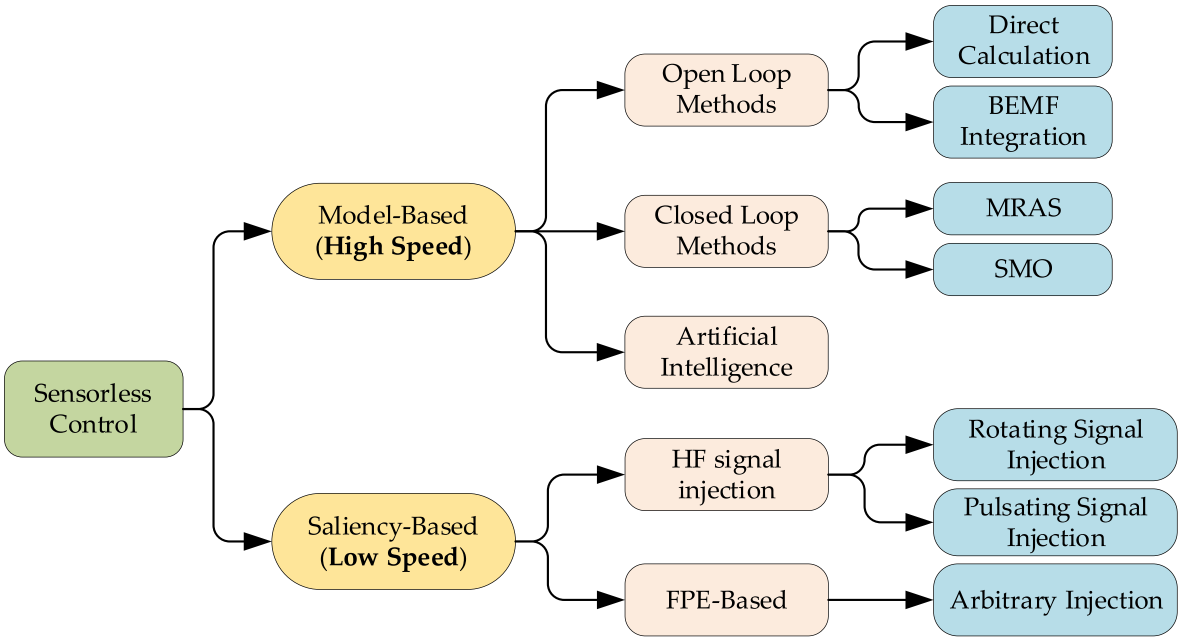

Figure 1. Categories of PMSM sensorless control methods.

Table 1. Position sensorless control algorithms.

Algorithms	Reference	Description
high frequency (HF) injection	[16–23]	The HF injection method is not reliant on the spatial protrusion of the tracking rotor rather than the mathematical equation of the motor, which addresses the sensitivity to the change in motor parameters and leads to a strong robustness. Yet the filter is needed, which has the defects of low signal-to-noise ratio and large phase lag in signal processing.
including direct calculation	[24–27]	This method does not depend on the speed of the motor, but it needs to increase the integral circuit and increase the hardware complexity and may bring additional integral error.
back-electromotive force (EMF)	[28–30]	The realization is simple, but the back EMF signal is small when the motor is low speed or static. The back EMF needs to be filtered, which will cause phase shift of the signal.
flux estimation	[31,32]	The rotor flux of the motor cannot be detected directly. It is necessary to measure the phase voltage and current of the motor, and to establish the function equation, which is directly related to the rotor flux without relying on the rotor speed. The calculation is large.
model reference adaptation system (MRAS)	[33–38]	The position observation is based on the accuracy of the reference model, and the accuracy of the parameters of the reference model itself directly affect the effectiveness of the identification.
sliding mode observer (SMO)	[39–42]	It can solve the problem that the motor is difficult to control at high speed and heavy load, and has strong robustness, but it needs a large amount of operation.

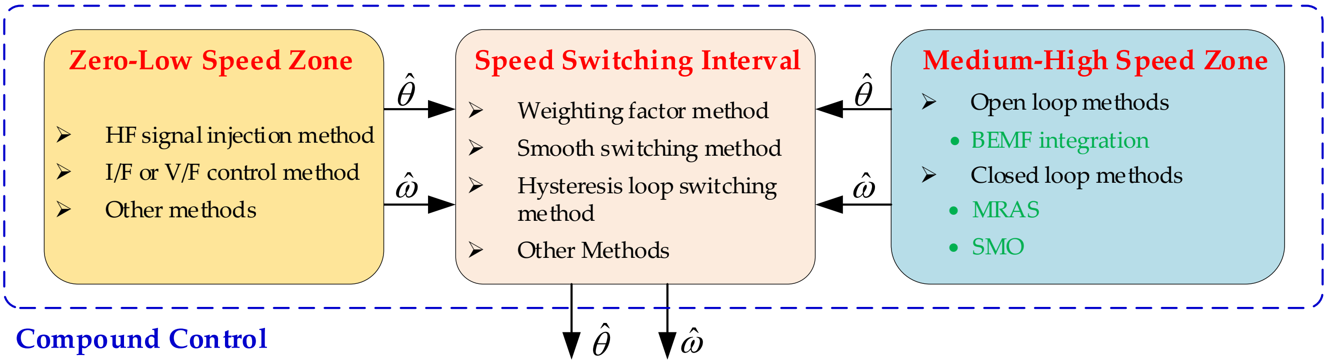

Figure 2. The block diagram of the compound control structure in full speed.

In addition to the conventional compound control algorithms above, there are also many special control algorithms in the full-speed range, such as compound control based on three-stage control [43–45] and compound control based on arbitrary injection [46,47].

The contribution of this paper is a classification of state-of-the-art compound position estimation methods and advances in sensorless control. The paper provides a complete overview of the advantages and disadvantages of HF-based, as well as IF-based, compound estimation techniques, which provides an effective guide for researchers working in this field.

The rest of this review paper is organized as follows. Section 2 introduces sensorless position estimate strategy for compound control based on the high-frequency injection method and Section 3 for compound control based on I/F control. Section 4 introduces the switching strategy in the full-speed range. Conclusions and future trends are drawn in Section 5.

2. Compound Control Based on High-Frequency Injection Method

High-frequency signal injection methods are generally divided into two categories. One is the high-frequency voltage injection method, and the other is the high-frequency current injection method [17]. As the high-frequency current injection method is difficult to control due to the high requirements of the current regulator used, the high-frequency voltage signal injection method is more commonly used. According to the different injection signals, high-frequency voltage injection methods are divided into two categories. One is the high-frequency rotary voltage injection, the other is the high-frequency pulse voltage injection. The former enables sensorless control of saliency-pole motors, and the latter is suitable for sensorless control of both saliency-pole and hidden-pole motors. A large number of researchers have made many improvements to traditional signal injection [18–23]. Therefore, the current system of high-frequency signal injection methods has been formed. Since this paper focuses on compound control, instead of giving a detailed account of each high-frequency signal injection method, two common high-frequency voltage signal injection methods have been selected for introduction.

The principle of the high-frequency voltage signal injection method is that when the motor is at standstill or running at low speed, the injection of a high-frequency voltage signal into the winding, due to the saliency of the motor, causes the feedback high-frequency signal to carry rotor position information.

1. High-frequency rotating injection method:

In general terms, the basic principle of this method is to add a high-frequency voltage excitation signal to the static coordinate system of the motor and to use the saliency of motors' own structural convex pole or saturated convex pole effect to produce a high-frequency current response. This current response contains both positive- and negative-phase sequence components, and only the phase of the negative-phase sequence high-frequency current component contains rotor position information. Therefore, appropriate signal processing techniques are required to extract rotor speed and position information by constructing suitable observer methods or the phase-locked loop method. The block diagram of the system structure is shown in Figure 3. The injected high-frequency voltage signal can be expressed as [8]

$$\begin{bmatrix} u_{\alpha h} \\ u_{\beta h} \end{bmatrix} = \begin{bmatrix} -U_{\mathrm{h}} \sin(\omega_{\mathrm{h}} t) \\ U_{\mathrm{h}} \cos(\omega_{\mathrm{h}} t) \end{bmatrix} \tag{1}$$

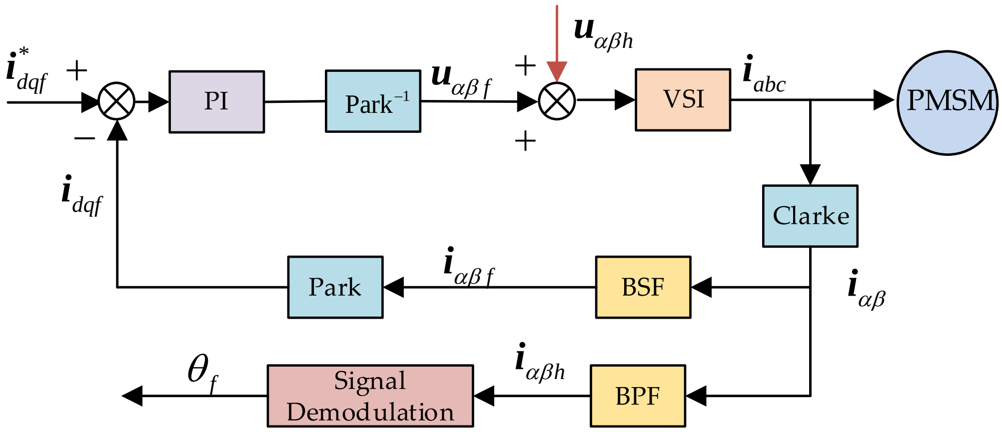

Figure 3. The control block diagram of the HF rotating injection method.

The high-frequency rotating injection method is insensitive to the uncertainty of motor parameters. However, its signal demodulation process is relatively complicated, the use of multiple filters deteriorates the dynamics of the system, and it is susceptible to multiple uncertainties leading to poor position-estimation accuracy.

2. High-frequency pulsating injection method:

The basic principle of this method is similar to that of the rotating high-frequency voltage signal method, except that the pulsating high-frequency voltage injection method only injects a high-frequency sinusoidal voltage signal into the d-axis of the estimated synchronous rotating coordinate system and produces a pulsating voltage vector in space. Figure 4a establishes the relationship between the estimated rotor and the actual rotor synchronous rotation coordinate system. In addition, in terms of the signal processing method for the feedback current, the pulsating high-frequency voltage injection method needs to multiply the high-frequency current component with the high-frequency sinusoidal signal for amplitude modulation, and then perform filtering and rotor position observation. The block diagram of the system structure is shown in Figure 4b. The injected high-frequency voltage signal can be expressed as [8].

$$\begin{bmatrix} \hat{u}_{\mathrm{dh}} \\ \hat{u}_{\mathrm{qh}} \end{bmatrix} = \begin{bmatrix} U_{\mathrm{h}} \cos(\omega_{\mathrm{h}} t) \\ 0 \end{bmatrix} \tag{2}$$

Compared with the high-frequency rotating injection method, the high-frequency pulsating signal injection method does not require the salient polarity of the motor and has the advantages of reliability, with inverter non-linearity and high accuracy in position identification. However, it has the problems of a long convergence time, poor dynamic performance and small stability range [19,20].

This section then provides an in-depth analysis of compound control based on the two widely used high-frequency signal injection methods mentioned above.

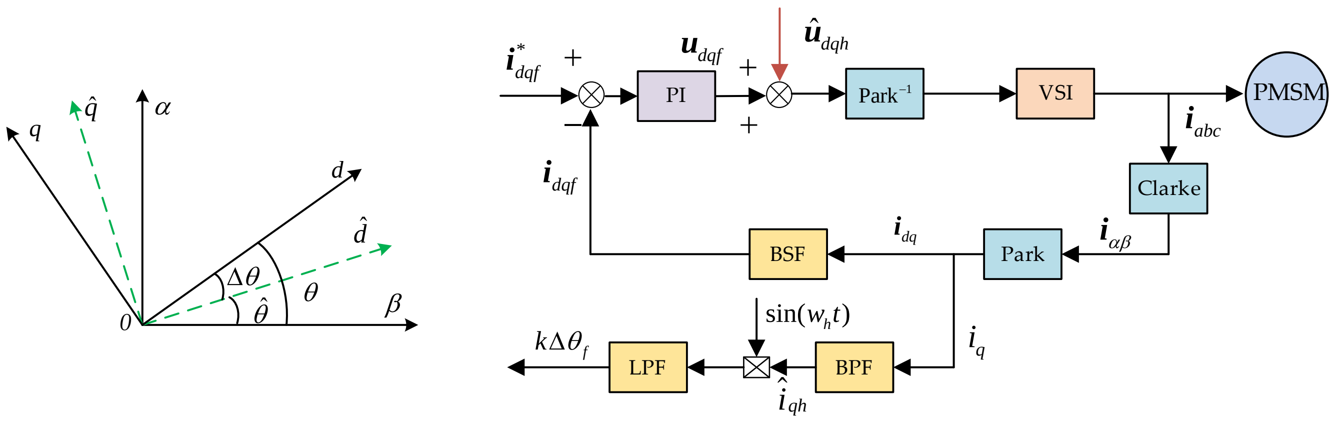

Figure 4. (**a**) The relationship between the estimated rotor and the actual rotor synchronous rotation coordinate system; (**b**) The control block diagram of the HF pulsating injection method.

2.1. HF Compounded with Model Reference Adaptive Method

The model reference adaptive system (MRAS) is a common method for estimating rotor positions based on the fundamental wave model method [33,34]. The basic principle of MRAS is to use the mathematical equations containing the parameters to be estimated as the adjustable model and the PMSM itself, which does not contain the unknown parameters, as the reference model. The output error of the two models is used to achieve the tracking of the adjustable model to the reference model by designing a suitable adaptive law to achieve the estimation of the rotor position and speed [35–37]. The basic structure is shown in Figure 5.

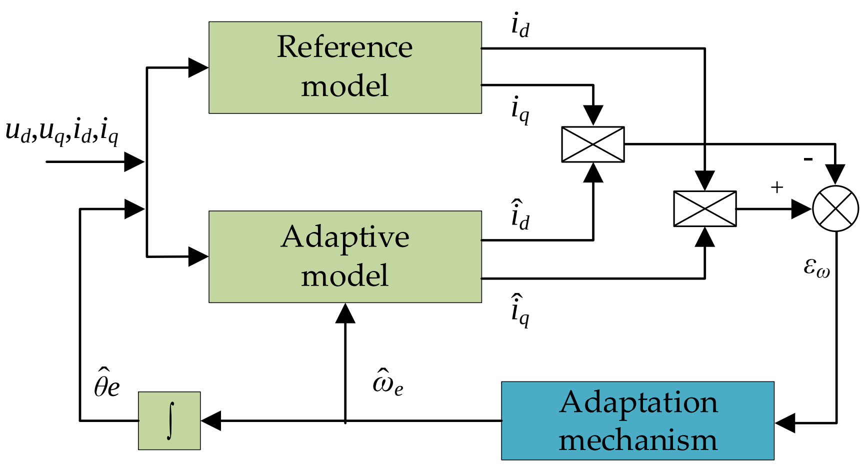

Figure 5. Block diagram of parallel structure MRAS.

In [48,49], Qin and Xu combined HF signal injection with MRAS in order to obtain rotor position estimates in the full-speed range. Rotor position and speed signals are obtained by the HF signal injection method at zero–low speeds, and by the model reference adaption method at medium and high speeds. The switching of the two algorithms is achieved by a switching method with weighting factors, which is described in detail separately in Section 4. In [50], the error term constructed using the HF pulse injection method was applied to correct the model reference adaptive observer, and the rapid dynamic response performance of the adaptive observer was combined with the steady-state accuracy of the HF injection method. The framework diagram of the compound system is shown in Figure 6.

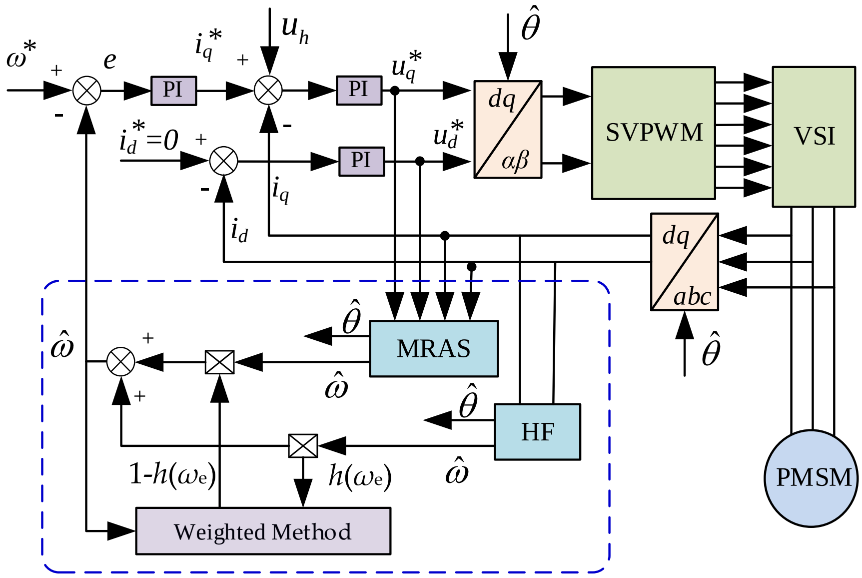

Figure 6. Block diagram of a compound control structure based on MRAS and HF.

The MRAS has the advantages of parameter adaption, structural simplicity and good steady-state performance [51]. As a result, it is often used in combination with HF for position estimation in the full-speed range. However, the performance of this algorithm depends on the selection of the reference model and the design of the adaptive law, which directly affect the stability and robustness of the algorithm, as well as the accuracy of the estimation. Therefore, the design of the adaptive law has been a problem that needs to be studied in depth in this method in order to obtain superior performance in the full-speed range [35]. In order to improve the robustness of this algorithm, the literature [36] proposes to combine the sliding mode algorithm with MRAS to improve the robustness of the system. In [52], Li introduced ADRC into the adaptive law design of MRAS to improve the estimation accuracy and increase the robustness of the system.

2.2. HF Compounded with Sliding Mode Observer

The Sliding Mode Observer (SMO) algorithm uses a switching characteristic that makes the structure of the system change over time, allowing the control to take on a discontinuous character [53,54]. The basic principle of the method is to build the SMO from a mathematical model of a permanent magnet synchronous motor and to design the sliding surface from the estimated error between the observed and actual currents [55,56]. By measuring the estimation error of the current, the back electromotive force is reconstructed and the rotor position and speed information is estimated using the back electromotive force. The basic structure is shown in Figure 7.

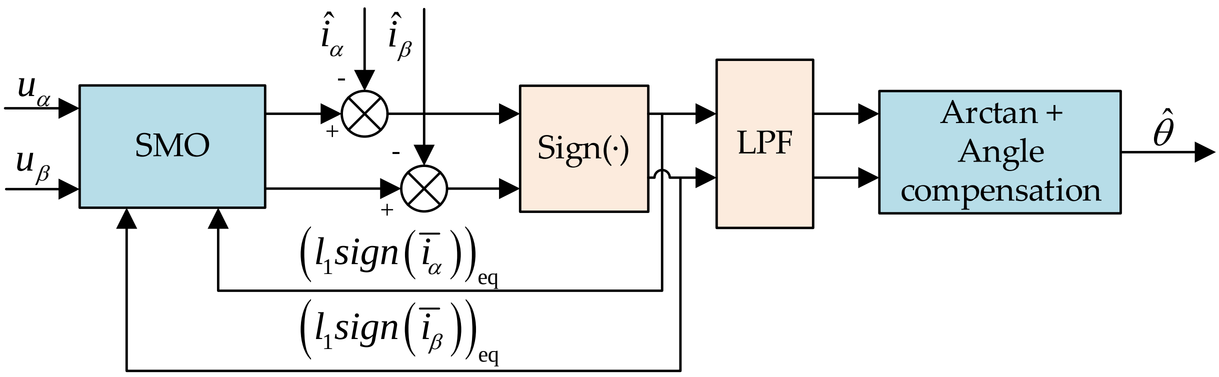

Figure 7. Block diagram of SMO.

In [57,58], the HF signal injection method was combined with SMO to determine the rotor position. The driver not only adopted a nonlinear adaptive SMO for the estimation of the rotor speed, but also conducted Lyapunov stability analysis to improve the low-speed and stationary performance of the drive. In [58], the running speed range of the motor was split into three sections, including a low-speed zone, transition zone and medium high-speed zone, so as to realize the smooth switching of the control method of the whole speed range of the motor, while verifying the sudden addition load and the discharge load of the transition area. In [59], a nonlinear sliding mode speed regulation scheme was proposed for IPMSM to be combined with the maximum torque amperometry trajectory. The global asymptotic stability of the controller and observer was ensured by Lyapunov stability analysis. As for IPMSM, Wang proposed a hybrid observation method based on a combination of the location error information of high-frequency signal injection and the anti-electric potential model method. The HF voltage signal of pulse vibration was injected during low-speed operation, and the medium–high-speed operation obtained the information on the position error through the anti-electric potential model SMO, thus normalizing the position error signal captured by the two methods and merging the information in a weighted way [60]. The scheme of the hybrid methods adopted in these papers is shown in Figure 8. Aiming at the compound control method based on rotational speed or position information fusion, it shows the disadvantages of high operation complexity and the difficulty in realization.

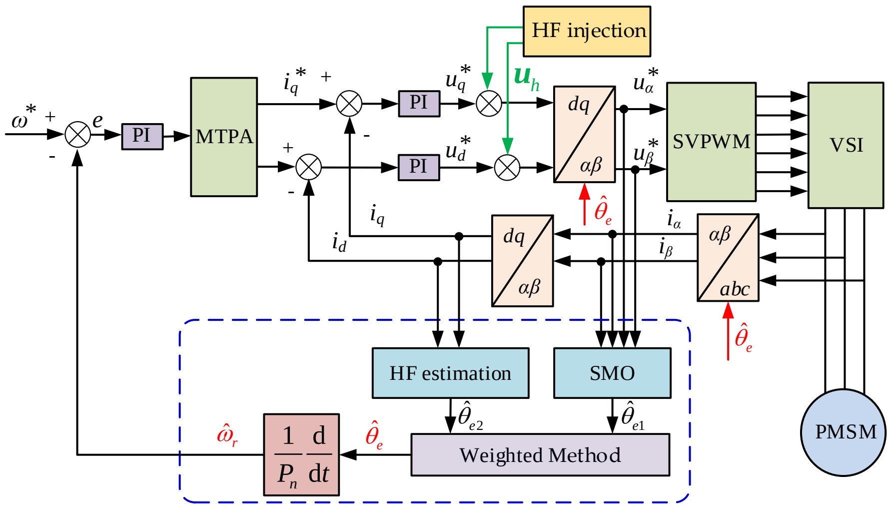

Figure 8. The block diagram of the rotor position hybrid observer based on HF and SMO.

2.3. HF Compounded with BEMF Integration Method or Flux Estimation

The BEMF integration method, or flux estimation, is an open-loop algorithm, which is different from the two-position sensorless algorithms already described above at medium and high speeds [61,62]. The key point of this algorithm is to obtain an accurate rotor magnetic chain vector and to use it to derive rotor position information. The stator voltage equation and the stator-rotor magnetic chain relationship in the α-β coordinate system of a permanent magnet synchronous motor are used for integration and inverse trigonometric operations to find the rotor position angle and speed [63].

$$\psi_f = \boldsymbol{\psi}_s - \boldsymbol{L}_{\alpha\beta}\boldsymbol{I}_s = \int (\boldsymbol{U}_s - R_s\boldsymbol{I}_s)\mathrm{d}t - \boldsymbol{L}_{\alpha\beta}\boldsymbol{I}_s \tag{3}$$

$$\theta_e = \arctan\frac{\boldsymbol{\psi}_{f\alpha}}{\psi_{f\beta}} \tag{4}$$

where $\boldsymbol{\psi}_f$ is the permanent magnet chain vector; $\boldsymbol{\psi}_s$ is the stator synthetic magnetic chain vector; $\boldsymbol{U}_s$ is the stator voltage vector; $\boldsymbol{I}_s$ is the stator current vector; $\boldsymbol{L}_{\alpha\beta}$ is the inductance matrix of the motor in the α-β coordinate system; and $\boldsymbol{\psi}_{f\alpha}$ and $\boldsymbol{\psi}_{f\beta}$ are the components of the rotor magnetic chain on the α-β axis, respectively. The basic structure is shown in Figure 9.

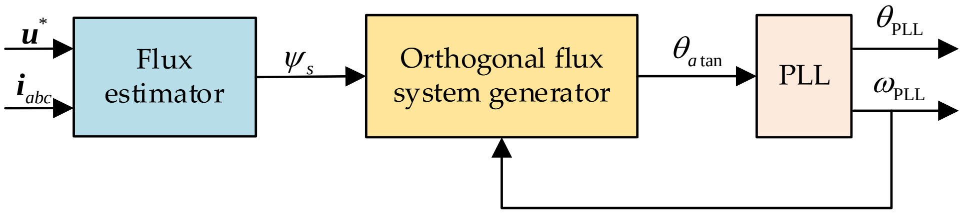

Figure 9. The block diagram of Flux Estimation.

In [64,65], a hybrid structure integrating flux observer and signal injection technology was proposed to make the rotor position signal independent of motor parameters at low and zero speed. In [66], a single Luenberger position observer compound control method based on the integration of standardized position error information was suggested. The standard position error signals were captured by square-wave voltage injection and the back-EMF model, respectively, at different speeds, and the information on the weighted fusion of the standardized position error signals in the transition region was collected through velocity information. In [67], when the motor remained up and running at low speeds, the real-time three-phase inductance of the motor was obtained by the rotating HF injection method, and the stator flux was obtained by combining the phase current. When the motor was running at high speeds, the back-EMF filter was applied to estimate the stator flux, according to which the DTC method based on the torque angle was combined, the motor operation was controlled, and the hysteresis method was used to ensure the smooth transition. In [68], through a combination of the EEMF and the HF signal injection method, the amplitude of the signal current was adjusted to maintain sufficient EEMF amplitude for mitigating interference. As the lower bound of the EEMF could be adjusted according to the degree of interference, signal setting was made easier. The scheme of the hybrid methods adopted in these papers is similar to Figure 8.

3. Compound Control Algorithm Based on I/F Control

I/F control is a frequency conversion speed control process to keep the current stable through the current closed loop, avoiding too much or too little current []. I/F control can directly control the torque current, which improves the ability to match the motor output torque with the load torque and can avoid low-frequency oscillation during motor operation. V/F control is similar to I/F control in that it is also a variable frequency speed control strategy, but in contrast to I/F control, V/F control is open loop for both speed and current, whereas I/F control is open loop for speed and closed loop for current. The schematic diagram for starting and running a permanent magnet synchronous motor via I/F control is shown in Figure 10.

At the initial start, the virtual synchronous coordinate system lags behind the synchronous coordinate system by a $\pi/2$ electrical angle. As the virtual synchronous coordinate system rotates, the motor rotor also starts to rotate with the virtual synchronous coordinate system. The motor output electromagnetic torque is determined by the phase difference between the two coordinate systems, and the motor output electromagnetic torque is shown as

$$T_e = \frac{3}{2} n_p \psi_f i_q^* \cos \theta_L \tag{5}$$

The equation for the torque balance of the motor during acceleration is

$$T_e - T_L = \frac{J}{n_p} \cdot \frac{\mathrm{d}\omega_{re}}{\mathrm{d}t} = \frac{J}{n_p} \cdot \frac{\mathrm{d}^2\theta_{re}}{\mathrm{d}t} \tag{6}$$

where i_q* is the given current; J is the rotational inertia; T_L is the load torque; and ω_{re} is the rotor electric angular velocity.

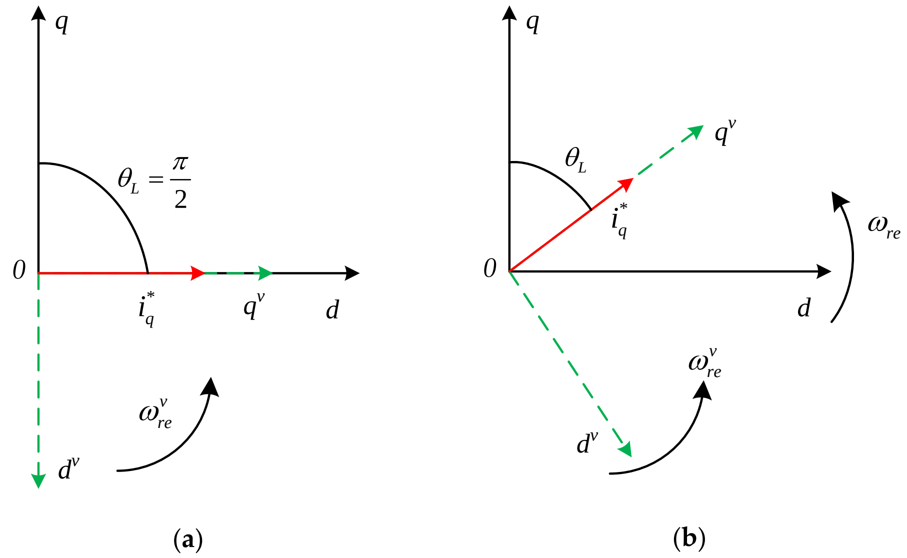

Figure 10. The phase relation of virtual synchronous frame and rotor synchronous frame in IF control. (**a**) Start state; (**b**) Running state.

3.1. I/F Compounded with Sliding Mode Observer

In [69,70], the I/F control method combined with a SMO composite control strategy was presented. In order to analyze the phase relationship of the virtual synchronous coordinate system and the rotor synchronous coordinate system used in the I/F control, the I/F control strategy of rotational speed open loop and current closed loop was adopted in the low-speed region of the motor. The adaptive SMO estimated the rotor flux by introducing the electric angular velocity. Based on I/F open-loop control theory, single-current closed-loop I/F control was achieved based on instantaneous reactive power, thus improving the current utilization [71]. The block diagram of the rotor position compound control methods based on I/F and SMO is shown in Figure 11.

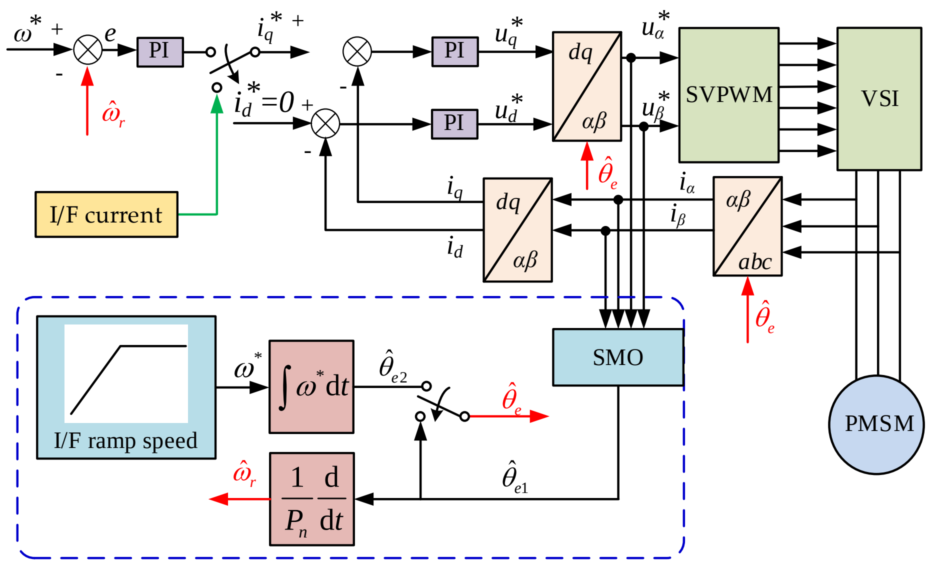

Figure 11. The block diagram of the rotor position compound control methods based on I/F and SMO.

3.2. I/F Compounded with Flux Obsever

In [72], a hybrid sensorless control strategy integrated with an improved flux linkage observer and the current-frequency (I-F) starting method was proposed. The I/F control method was utilized for the stable startup and strong antijamming capability, and the improved flux linkage observer based on the sliding-mode compensator is designed for the closed-loop sensorless operation. An adaptive transition algorithm was designed in order to achieve smooth operation between the two different control schemes.

4. Switching Methods

From the above sections, it can be found that the current compound control methods mainly use one or more zero–low-speed control methods combined with one or more methods of position sensorless control at medium and high speeds to achieve the full-speed range of the compound control technology, so how to achieve a smooth transition and switching between the two speed detection methods is an extremely important part of whether the compound control can achieve reliable operation [73]. The switching control algorithm between the two control methods is also the focus of this paper.

4.1. Weighting Factor Method

The basic principle of the weighted coefficient switching method is that when the rotor speed is above the upper limit of the switching interval, the medium–high speed control method is used for control; when the speed is below the lower limit of the switching interval, the position sensorless control method at zero–low speed is used for control; and when the estimated speed is within the switching interval, the weighted value of the results of the two algorithms is used to ensure smooth switching of the two methods. At the same time, the lower speed limit in the switching zone should be higher than the minimum speed at which the control algorithm can operate at medium and high speeds, while the upper speed limit in the switching zone should be lower than the maximum speed at which the control algorithm can start itself at zero–low speed. To ensure that there are no jumps in position and speed signals in the switching zone, the two methods are required to have essentially the same speed and position errors in the switching zone [5,60]. The block diagram of the system structure is shown in Figure 12. The estimation equation for the rotor speed is

$$\hat{n} = W_{\mathrm{h}}\hat{n}_{\mathrm{h}} + (1 - W_{\mathrm{h}})\hat{n}_{\mathrm{m}} \tag{7}$$

where $\hat{n}$ is the estimated speed of the compound; are the lower and upper limits of the speed switching interval respectively; and a and b are estimated speeds at zero–low speed and medium–high speed, respectively. The weighting factor W_{h} is

$$W_{\mathrm{h}} = \begin{cases} 1, & \hat{n} \leqslant n_1 \\ \frac{n-n_2}{n_1-n_2}, & \hat{n}_1 < n < n_2, \\ 0, & \hat{n} \geqslant n_2. \end{cases} \tag{8}$$

Although this weighted coefficient method has a simple structure and is easy to implement, in practical applications, in order to achieve reliable switching during speed changes, both algorithms need to run all the time, resulting in a large amount of wasted hardware and software resources, and also causing an impact on the system control performance due to the constant injection of high-frequency signals. In [74], Zhao proposed an improvement scheme: under the premise of ensuring the upper and lower limits of the switching interval remain unchanged, based on the basis of the variable weighted switching algorithm, the working interval of the two algorithms is reduced, while providing sufficient margin for the convergence of the algorithms, and the speed and rotor position identified by the other algorithm in real time when each algorithm starts working is used as the initial value for the identification of the new working algorithm in order to enable the algorithm that suddenly switches to the working state to quickly converge to a stable value. The lower limit of the switching interval for both algorithms is set to 100 r/min, and the upper limit is set to 200 r/min. On top of this, the speed of the MRAS method is additionally set to 50 r/min at the start of the speed rise phase, and the speed of the pulse vibration injection method is set to 300 r/min at the start of the operation. The operation of the improved switching algorithm in each speed interval is shown in Figure 13.

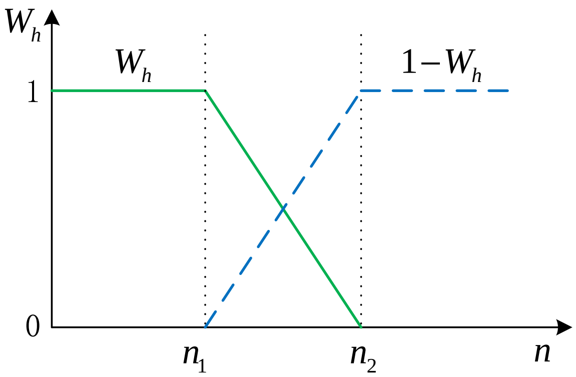

Figure 12. The block diagram of the system structure for weighting factor method.

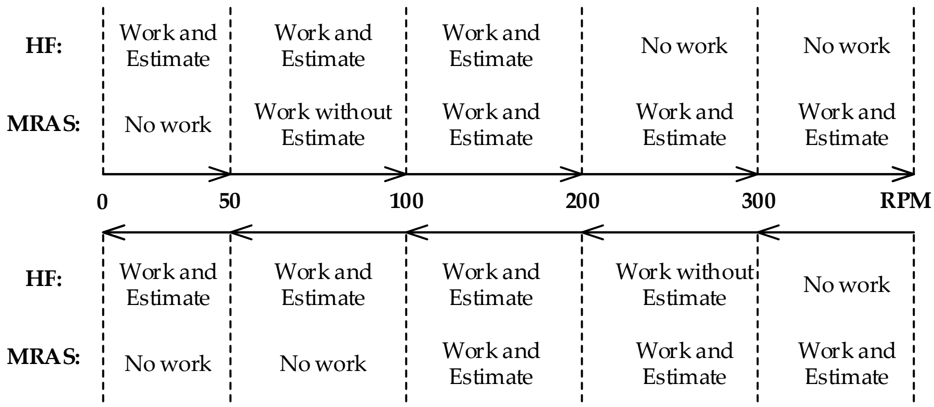

Figure 13. Operations of high-frequency pulse injection method and MRAS in each speed interval after improvement.

4.2. Smooth Switching Method

The smooth switching algorithm is mostly used in the control strategy of I/F start-up. The I/F control uses a virtual synchronous coordinate system, which has a phase difference, θ_L, between it and the rotor synchronous coordinate system [69,70]. The process of smooth switching control strategy is actually the process of adjusting the phase difference θ_L from an acute angle to close to zero. The phase angle difference θ_L during I/F control preparation for switching cannot be equal to zero, otherwise it will cause the motor to miss-step [71,72,75]. The ideal control strategy is shown in Figure 14.

The traditional smooth switching strategy is actually a strategy of smooth switching by gradually adjusting the given angle of the virtual synchronous coordinate system in the IF control. However, due to the "torque-work angle self-balancing" principle, the virtual synchronous coordinate system can never "catch up" with the rotor synchronous coordinate system. In order to solve this problem, in [8], Liu proposed a smooth switching strategy by adjusting the amplitude of the virtual q^{v}-axis current given indirectly to adjust the phase difference θ between the two coordinate systems at heavy load, and by adjusting the virtual q^{v}-axis and virtual d-axis current given simultaneously at no load or light load. This improved switching strategy has a wider range of application, and at the same time, in this improved switching strategy, the synthetic current vectors of the q^v and d^v axes have a larger phase difference with the q-axis of the rotor synchronous coordinate system, such that this switching strategy is more resistant to disturbances and has a lower risk of motor miss-steps. The improved switching strategy is shown in Figure 15.

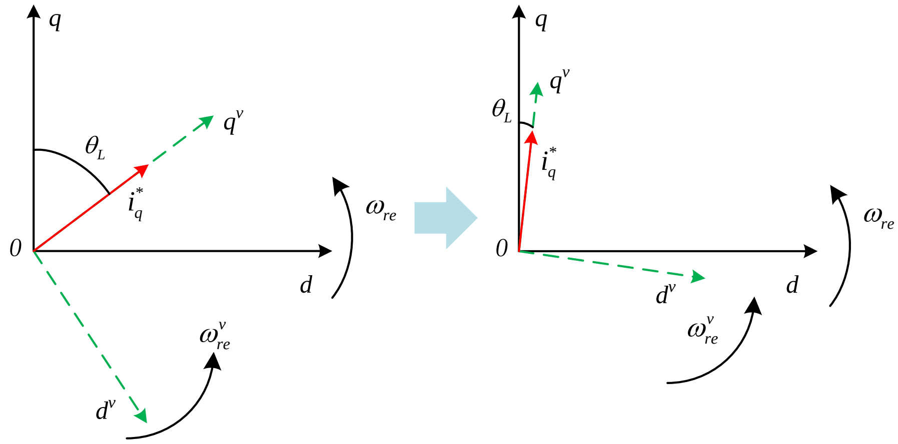

Figure 14. The block diagram of the ideal control strategy for smooth switching method.

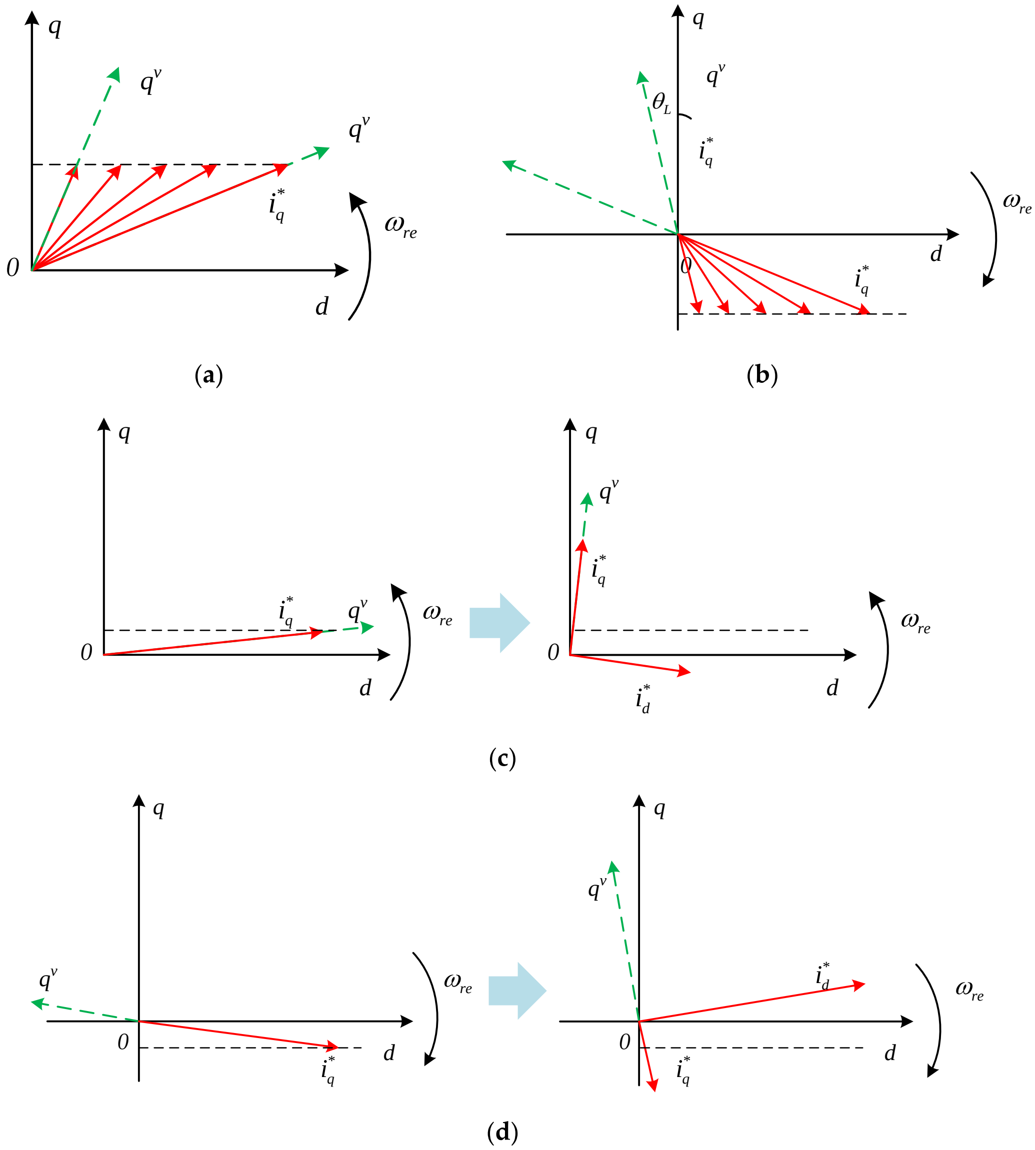

Figure 15. The block diagram of the improved smooth switching strategy. (**a**) Motor positive rotation under heavy load; (**b**) Motor negative rotation under heavy load; (**c**) Motor positive rotation under light load; (**d**) Motor negative rotation under light load.

4.3. Hysteresis Loop Switching Method

The hysteresis loop switching strategy is shown in Figure 16. When the speed rises to $|\omega_{eH}|$, the estimated position is quickly switched from the position sensorless estimation algorithm at zero–low speed to the position sensorless estimation algorithm at medium and high speed within a certain time T_{sw}. The switching process uses a smooth transition strategy as

$$\hat{\theta}_{e} = g_{h}\hat{\theta}_{h} + (1 - g_{h})\hat{\theta}_{m} \tag{9}$$

$$\hat{\omega}_{e} = g_{h}\hat{\omega}_{h} + (1 - g_{h})\hat{\omega}_{m} \tag{10}$$

where $\hat{\theta}_{hf}$, $\hat{\omega}_{hf}$ are the estimated position and speed obtained by the zero–low-speed sensorless estimation algorithm, respectively; and $g_{hf} = t/T_{sw}$, where $0 \leq t \leq T_{sw}$. The zero–low-speed sensorless estimation algorithm can be removed when all positions estimated by the medium- and high-speed sensorless estimation algorithm are used in order to reduce losses, noise, etc. To avoid the problem of switching back and forth between the two methods due to speed fluctuations, a hysteresis loop strategy is designed so that the position-free estimation algorithm at medium and high speeds is switched to the position sensorless estimation algorithm at zero–low speed, only when the speed is below $|\omega_{eL}|$. As $|\omega_{eL}|<|\omega_{eH}|$, it can avoid switching back and forth between the two methods at two switching points and improve the smoothness of speed operation at the switching point [76,77].

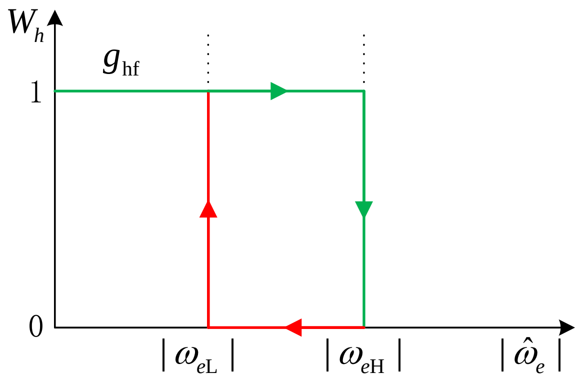

Figure 16. The block diagram of Hysteresis loop switching method.

5. Conclusions

This article reviews the two main types of state-of-the-art compound control based on high-frequency signal injection, and compound control based on IF algorithms without position sensors and their switching algorithms. The advantages and disadvantages of compound control combined with MRAS, SMO, BEMF, et al. are presented under compound control based on the HF signal injection method and I/F control, and the position estimation process is illustrated with examples. In addition, the advantages and disadvantages of the various switching algorithms in the compound control algorithm are presented. The following points can be drawn from the content of the sections set out above:

1. The high-frequency signal injection method has many advantages, but there are also problems of long convergence time, poor dynamic performance and small stability range. For compound control, the advantages of the high-frequency signal injection method inherit many disadvantages, which can have more or less impact on the estimation accuracy and other aspects in the compound control process. Therefore more advanced high-frequency signal injection methods should be studied to improve the reliability of the dynamic range of motor compound control estimation.
2. I/F control is simple in structure, easy to implement, and has the advantages of smooth start-up and no current overcharge. It is the current start-up strategy for most position sensor-free control at medium and high speeds. However, the basic

I/f control strategy is an open-loop scheme with disadvantages, such as the current amplitude and frequency cannot be automatically adjusted, and there is a tendency to lose steps, and the speed is easily disturbed, so its improvement will largely improve the performance of the compound control.

3. There is a wide variety of control strategies for position sensorless control at high speeds, each with its own advantages, but also some shortcomings. So, the improvement of such algorithms will greatly improve the performance of the current compound control.
4. Switching algorithms play a pivotal role in compound control. In the current research field of compound control, whether based on HF control or I/F control, switching strategies are required. Most of the switching algorithms commonly used today have the advantages of, for example, simpler methods and relatively stable algorithm switching, but their switching smoothness is not ideal, which means that the existing switching algorithms should be improved to achieve smoother and more stable switching, or smoother and more stable switching algorithms should be developed to meet the current high demand for motor position estimation.

Author Contributions: Conceptualization, Y.L. and H.H.; methodology, Y.L. and P.S.; investigation, H.H.; data curation, H.H.; writing—original draft preparation, Y.L. and H.H.; writing—review and editing, Y.L. and P.S.; supervision, Y.L.; project administration, Y.L.; funding acquisition, Y.L. and P.S. All authors have read and agreed to the published version of the manuscript.

Funding: This work is supported by the National Natural Science Foundation of China (Grant No. 51705213), supported by the Opening Project of Automotive New Technique of Anhui Province Engineering Technology Research Center (Grant No. QCKJ202201A) and supported by the Opening Project of National Engineering Laboratory of Energy-saving Motor & Control Technique of Anhui University (Grant No. KFKT202215).

Data Availability Statement: Not applicable.

Conflicts of Interest: The authors declare no conflict of interest.

References

1. Li, Y.; Wu, H.; Xu, X.; Sun, X.; Zhao, J. Rotor Position Estimation Approaches for Sensorless Control of Permanent Magnet Traction Motor in Electric Vehicles: A Review. *World Electr. Veh. J.* **2021**, *12*, 9. [CrossRef]
2. Jiang, H.B.; Li, A.X.; Ma, S.D.; Chen, L. Design and performance analysis of airflow energy recovery device of electric vehicle. *J. Jiangsu Univ.* **2017**, *38*, 125–132.
3. Liu, C.H.; Luo, Y.X. Overview of Advanced Control Strategies for Electric Machines. *Chin. J. Electr. Eng.* **2017**, *3*, 53–61.
4. Li, S.Q.; Ding, X.M.; Yu, B. Optimal control strategy of efficiency for dual motor coupling drive system of pure electric vehicle. *J. Jiangsu Univ.* **2022**, *43*, 1–7.
5. Zhang, H.; Liu, W.G.; Chen, Z.; Mao, S.; Meng, T.; Peng, J.C.; Jiao, N.F. A Time-Delay Compensation Method for IPMSM Hybrid Sensorless Drives in Rail Transit Applications. *IEEE Trans. Ind. Electron.* **2019**, *66*, 6715–6726. [CrossRef]
6. Li, Y.; Wu, H.; Zhang, B.H. Frontier techniques and prospect of in-wheel motor for electric vehicle. *J. Jiangsu Univ.* **2019**, *40*, 261–268.
7. Xue, H.T.; Zhou, Y.; Wang, M.; Li, Z.X. Fault diagnosis method for in-wheel motor based on wolf pack algorithm. *J. Jiangsu Univ.* **2019**, *40*, 579–584.
8. Liu, J.L.; Xiao, F.; Shen, Y.; Mai, Z.Q.; Li, C.R. Position-Sensorless Control Technology of Permanent-Magnet Synchronous Motor-a Review. *Trans. China Electrotech. Soc.* **2017**, *32*, 76–88.
9. Li, J.M.; He, R. Optimization design and performance analysis of dual-rotor in-wheel motor based on parameter sensitivity. *J. Jiangsu Univ.* **2020**, *41*, 640–647.
10. Sun, X.D.; Cao, J.H.; Lei, G.; Guo, Y.G.; Zhu, J.G. Speed Sensorless Control for Permanent Magnet Synchronous Motors Based on Finite Position Set. *IEEE Trans. Ind. Electr.* **2020**, *67*, 6089–6100. [CrossRef]
11. Wu, D.R.; Tian, S.P. New control strategy of motor for pure electric vehicle based on TLGI technology. *J. Jiangsu Univ.* **2021**, *42*, 9–14.
12. Guo, J.G.; Dog, H.X.; Sheng, W.H.; Tu, C. Optimum control strategy of regenerative braking energy for electric vehicle. *J. Jiangsu Univ.* **2018**, *39*, 132–138.
13. Zhang, L.; Zhu, X.Y.; Gao, J.; Mao, Y. Design and Analysis of New Five-Phase Flux-Intensifying Fault-Tolerant Interior-Permanent-Magnet Motor for Sensorless Operation. *IEEE Trans. Ind. Electron.* **2020**, *67*, 6055–6065. [CrossRef]

14. Wang, G.; Valla, M.; Solsona, J. Position sensorless permanent magnet synchronous machine drives—A review. *IEEE Trans. Ind. Electron.* **2019**, *67*, 5830–5842. [CrossRef]
15. Mohan, H.; Pathak, M.K.; Dwivedi, S.K. Sensorless control of electric drives–a technological review. *IETE Tech. Rev.* **2020**, *37*, 504–528. [CrossRef]
16. Lin, T.C.; Zhu, Z.Q. Sensorless operation capability of surface-mounted permanent-magnet machine based on high-frequency signal injection methods. *IEEE Trans. Ind. Appl.* **2015**, *51*, 2161–2171. [CrossRef]
17. Liu, Y.; Zhou, B.; Li, S.; Feng, Y. Initial Rotor Position Detection of Surface Mounted Permanent Magnet Synchronous Motor. *Proc. CSEE* **2011**, *31*, 48–54.
18. Liu, J.M.; Zhu, Z.Q. Sensorless control strategy by square aveform high-frequency pulsating signal injection into stationary reference frame. *IEEE J. Emerg. Sel. Top. Power Electron.* **2014**, *2*, 171–180. [CrossRef]
19. Zhou, T.; Jiang, Q. Overview of Sensorless Control Technology for Full Speed Range Permanent Magnet Synchronous Motors. *Electron. Sci. Technol.* **2021**, *34*, 59–69.
20. Xu, X.; Mi, J.; Wang, F.; Ma, S.D.; Tao, T. Design of differential braking control system of travel trailer based on multi-objective PID. *J. Jiangsu Univ.* **2020**, *41*, 172–180.
21. Yoon, Y.D.; Sul, S.K.; Morimoto, S.; Ide, K. High-Bandwidth Sensorless Algorithm for AC Machines Based on Square-Wave-Type Voltage Injection. *IEEE Trans. Ind. Appl.* **2011**, *47*, 1361–1370. [CrossRef]
22. Lu, J.D.; Liu, J.L.; Wei, L.C. Estimation of the Initial Rotor Position for Permanent Magnet Synchronous Motors. *Trans. China Electrotech. Soc.* **2015**, *30*, 105–111.
23. Zhou, Y.J.; Cai, M.F. Initial rotor position inspection of PMSM based on rotating high frequency voltage signal injection. *Electr. Mach. Control.* **2010**, *14*, 68–72.
24. Chen, S.H.; Liu, G.; Zhu, L.Q. Sensorless Start-Up Control Strategy for a 315 kW High-Speed Magnetic Suspension BLDC Motor with Small Inductance and Non-ideal Back-EMF. *IEEE Trans. Ind. Electron.* **2018**, *66*, 1703–1714. [CrossRef]
25. Damodharan, P.; Vasudevan, K. Sensorless Brushless DC Motor Drive Based on the Zero-Crossing Detection of Back Electromotive Force (EMF) From the Line Voltage Difference. *IEEE Trans. Energy Convers.* **2010**, *25*, 661–668. [CrossRef]
26. Zhang, G.Q.; Wang, G.L.; Xu, D.G.; Fu, Y.; Ni, R.G. Adaptive Notch Filter Based Rotor Position Estimation for Interior Permanent Magnet. *Proc. CSEE.* **2016**, *36*, 2521–2527.
27. Wang, D.F.; Zhu, Y.Q.; Jin, Y.; Liu, Z.Q. A novel research on detecting position of brushless DC motors. *Trans. China Electrotech. Soc.* **2013**, *28*, 139–144.
28. Shen, J.X.; Iwasaki, S. Sensorless control of ultrahigh-speed PM brushless motor using PLL and third-harmonic back EMF. *IEEE Trans. Ind. Electron.* **2006**, *53*, 421–428. [CrossRef]
29. Wang, D.F.; Zhu, Y.Q.; Jin, Y.; Zhao, G.Y. Tentative Strategy of Starting Sensorless BLDCM with the Method of Integrating the Back EMF. *Trans. China Electrotech. Soc.* **2012**, *27*, 178–184.
30. Chen, Z.Q.; Tomita, M.; Doki, S. An extended electromotive force model for sensorless control of interior permanent- magnet synchronous motors. *IEEE Trans. Ind. Electron.* **2003**, *50*, 288–295. [CrossRef]
31. Lee, K.G.; Lee, J.S.; Lee, K.B. Wide-range sensorless control for SPMSM using an improved full-order flux observer. *J. Power Electron.* **2015**, *15*, 721–729. [CrossRef]
32. Qiu, T.F.; Wen, X.H.; Zaho, F.; Wang, Y.X. Design Strategy of Permanent Magnet Flux Linkage Adaptive Observer for Permanent Magnet Synchronous Motor. *Proc. CSEE* **2015**, *35*, 2287–2294.
33. Zhu, Y.; Cheng, M.; Hua, W.; Zhang, B.F.; Wang, W. Sensorless control for electrical variable transmission based on sliding mode model reference adaptive system. *Trans. China Electrotech. Soc.* **2015**, *30*, 64–72.
34. Rai, R.; Shukla, S.; Singh, B. Electromagnetic Torque-Based Model Reference Adaptive System Speed Estimator for Sensorless Surface Mount Permanent Magnet Synchronous Motor Drive. *IEEE Trans. Ind. Inform.* **2020**, *16*, 4714–4725. [CrossRef]
35. Hu, W.H.; Wang, Y.; Li, M.X.; Li, M.; Wang, Z.A. Research on sensorless control strategy of direct drive multiphase PMSG wind power generation system based on MRAS. *Power Syst. Prot. Control.* **2014**, *42*, 118–124.
36. Li, Y.H.; Zhao, Y.Q. Path tracking of 4WIS autonomous vehicle based on double-layer control strategy. *J. Jiangsu Univ.* **2022**, *43*, 386–393.
37. Zhang, H.S.; Wang, P.; Han, B.C. Rotor Position Measurement for High-speed Permanent Magnet Synchronous Motors Based on Fuzzy PI MRAS. *Proc. CSEE* **2014**, *34*, 1889–1896.
38. Yao, X.L.; Ding, D.D.; Yang, Y.; Ge, W.J.; Wu, M.Y. Failure compensation control design of adaptive actuator for vehicle robot driver. *J. Jiangsu Univ.* **2021**, *42*, 642–647.
39. Xu, B.; Shen, X.K.; Ji, W.; Shi, G.D. Adaptive Nonsingular Terminal Sliding Model Control for Permanent Magnet Synchronous Motor Based on Disturbance Observer. *IEEE Access* **2018**, *6*, 48913–48920. [CrossRef]
40. Zhang, X.; Guo, L.L.; Yang, S.Y.; Cao, R.X. Speed Sensorless Control of Permanent Magnet Synchronous Generators. *Proc. CSEE* **2014**, *34*, 3440–3447.
41. Su, J.Y.; Li, T.C.; Yang, G.J. PMSM sensorless control based on four-order hybrid sliding mode observer. *Proc. CSEE* **2009**, *29*, 98–103.
42. Zhao, Y.; Qiao, W.; Wu, L. Improved Rotor Position and Speed Estimators for Sensorless Control of Interior Permanent- Magnet Synchronous Machines. *IEEE J. Emerg. Sel. Top. Power Electron.* **2014**, *2*, 627–639. [CrossRef]

43. Zhang, Z.Y.; Lin, M.Y.; Zhou, G.Q. Anti-reverse rotation startup and smoothly switching of sensorless brushless DC motor. *Trans. China Electrotech. Soc.* **2009**, *24*, 26–32.
44. Wu, C.; Qi, R.; Li, B.Q.; Ma, D.L. Whole Speed Range Sensorless Control of Permanent Magnet Synchronous Motor Considering Saturation Effect. *Trans. China Electrotech. Soc.* **2017**, *32*, 171–179.
45. Chen, S.Y.; Pi, Y.G. Position Sensorless Control for Permanent Magnet Synchronous Motor Based on Sliding Mode Observer and Sliding Mode Controller. *Trans. China Electrotech. Soc.* **2016**, *31*, 108–117.
46. Wang, Z.; Lu, K.; Blaabjerg, F. A simple startup strategy based on current regulation for back-EMF-based sensorless control of PMSM. *IEEE Trans. Power Electron.* **2012**, *27*, 3817–3825. [CrossRef]
47. Barnard, F.J.; Villet, W.T.; Kamper, M.J. Hybrid active-flux and arbitrary injection position sensorless control of reluctance synchronous machines. *IEEE Trans. Ind. Appl.* **2015**, *51*, 3899–3906. [CrossRef]
48. Qin, F.; He, Y.K.; Jia, H.P. Investigationn of the Sensorless Control for PMSM Based on a Hybird Rotor Position Self-Sensing Approach. *Proc. CSEE* **2007**, *27*, 12–17.
49. Xu, H.Z.; Xie, S.Y.; Zhang, L.S.; Wang, S.L. Investigation of hybrid sensorless control approach for dualrotor PMSM. *Electr. Mach. Control.* **2012**, *16*, 12–16.
50. Antti, P.; Marko, H. Adaptation of motor parameters in sensorless PMSM drives. *IEEE Trans. Ind. Appl.* **2009**, *45*, 203–212.
51. Jiang, H.B.; Zhu, C.; Tang, B.; Yin, C.H.; Hua, Y.F.; Xie, J. Lateral stability control of ECHBPS commercial vehicle based on extension active disturbance rejection. *J. Jiangsu Univ.* **2021**, *42*, 166–172.
52. Li, Y.; Hu, H.; Qin, Z.C.; Wu, H. Sensorless control of permanent magnet in-wheel motor based on improved model reference adaptive strategy. *J. Automot. Saf. Energy* **2022**, *13*, 560–570.
53. Yang, M.H.; Li, S.Q.; Li, Z.; Feng, B.; Li, J. Active disturbance rejection controller of direct torque for permanent magnet synchronous motor based on super-twisting sliding mode. *J. Jiangsu Univ.* **2022**, *43*, 680–684, 696.
54. Jiang, H.B.; Cao, F.G.; Zhu, W.W. Control method of intelligent vehicles cluster motion based on SMC. *J. Jiangsu Univ.* **2018**, *39*, 385–390.
55. Chen, M.S.; Hwang, Y.R.; Tomizuka, M. A state-dependent boundary layer design for sliding mode control. *IEEE Trans. Autom. Control.* **2010**, *47*, 1677–1681. [CrossRef]
56. Zhang, J.C.; Wang, L.M.; Zou, X.J.; Song, W. Optimization control strategy of driving torque for slope-crossing of pure electric vehicles. *J. Jiangsu Univ.* **2021**, *42*, 506–512.
57. Wang, G.L.; Li, Z.M.; Zhang, G.Q.; Yu, Y. Quadrature PLL-Based High-Order Sliding-Mode Observer for IPMSM Sensorless Control with Online MTPA Control Strategy. *IEEE Trans. Energy Convers.* **2013**, *28*, 214–224. [CrossRef]
58. Li, R. *Research on the Sensorless Control. Technique of Permanent Magnet Synchronous Motor*; Zhejiang University: Hangzhou, China, 2012.
59. Gilbert, F.; Rahman, M.F. Sensorless sliding-mode MTPA control of an IPM synchronous motor drive using a sliding-mode observer and HF signal injection. *IEEE Trans. Ind. Electron.* **2010**, *57*, 1270–1278.
60. Wang, G.L.; Yang, R.F.; Xu, D.G. DSP-Based Control of Sensorless IPMSM Drives for Wide-Speed-Range Operation. *IEEE Trans. Ind. Electron.* **2013**, *60*, 720–727. [CrossRef]
61. Zhou, L.Y.; Wang, S.J. Torque control of BLDCM based on predictive current control. *J. Jiangsu Univ.* **2015**, *36*, 79–86.
62. Gupta, N.; Pandey, D.A.K. *A Review: Sensorless Control of Brushless DC Motor*; Esrsa Publications: Gandhinagar, India, 2012.
63. Boldea, I.; Paicu, M.C.; Andreescu, G.D.; Blaabjerg, F. Active flux" DTFC-SVM sensorless control of IPMSM. *IEEE Trans. Energy Convers.* **2009**, *24*, 314–322. [CrossRef]
64. Silva, C.; Asher, G.M.; Sumner, M. Hybrid rotor position observer for wide speed-range sensorless PM motor drives including zero speed. *IEEE Trans. Ind. Electron.* **2006**, *53*, 373–378. [CrossRef]
65. Andreescu, G.D.; Pitic, C.I.; Blaabjerg, F.; Boldea, I. Combined Flux Observer with Signal Injection Enhancement for Wide Speed Range Sensorless Direct Torque Control of IPMSM Drives. *IEEE Trans. Energy Convers.* **2008**, *23*, 393–402. [CrossRef]
66. Zhang, G.Q.; Wang, G.L.; Xu, D.G.; Yu, Y. Hybrid Sensorless Control Based on Single Position Observer Using Error Combination for Interior Permanent Magnet Synchronous Machine Drives. *Proc. CSEE* **2017**, *37*, 6077–6082.
67. Qiu, X.; Huang, W.X.; Bu, F.F. Sensorless direct torque control of interior permanent magnet synchronous machines over wide speed range. *Trans. China Electrotech. Soc.* **2014**, *29*, 92–99.
68. Ohnuma, T.; Makaino, Y.; Saitoh, R. Adaptive signal injection method combined with EEMF based position sensorless control of IPMSM drives. *IEEJ J. Ind. Appl.* **2014**, *4*, 914–918.
69. Song, G.Y.; Li, J.L. A Sensorless Control for PMSM with combined IF and Improved Sliding Mode Observer. *Electr. Mach. Control.* **2020**, *24*, 63–72.
70. Liu, J.L.; Xiao, F.; Mai, Z.Q.; Gao, S.; Yu, X.W. Hybrid Position-Sensorless Control Scheme for PMSM Based on Combination of IF Control and Sliding Mode Observer. *Trans. China Electrotech. Soc.* **2018**, *33*, 919–929.
71. Wang, M.; Yang, J.Q.; Zhang, X.; Zhu, C.S. An I/f Control Method with Closed-loop Regulation of Current Vector for Surface Permanent Magnet Synchronous Motor Drives. *Proc. CSEE* **2015**, *35*, 2513–2521.
72. Tang, Q.P.; Chen, D.X.; He, X.N. Integration of Improved Flux Linkage Observer and I-f Starting Method for Wide-Speed-Range Sensorless SPMSM Drives. *IEEE Trans. Power Electron.* **2020**, *35*, 8374–8383. [CrossRef]
73. Tao, W.; Liu, Z.Q. Seat suspension control of wheel loader based on damping state switching. *J. Jiangsu Univ.* **2019**, *40*, 504–510.
74. Zhao, Q.J.; Liao, Z.L.; Zhang, Y.Y.; Cai, L.C. Research on Position Sensorless Control of Hub Motor in Full Speed Range. *Acta Armamentarii* **2019**, *40*, 915–926.

75. Wu, D.D.; Ge, Q.; Xu, X.F.; Qiu, B.Y. Grid-connected control strategy of virtual synchronous generator based on virtual power. *J. Jiangsu Univ.* **2022**, *43*, 458–463.
76. Panin, S.V.; Bogdanov, A.A.; Eremin, A.V.; Buslovich, D.G.; Alexenko, V.O. Estimating Low- and High-Cyclic Fatigue of Polyimide-CF-PTFE Composite through Variation of Mechanical Hysteresis Loops. *Materials* **2022**, *15*, 4656. [CrossRef]
77. Wu, C.; Fu, Z.J.; Sun, M.X.; Liu, Z. Sensorless Control of PMSM in All Speed Range Based on Extended State Observer for Load Toque Compensation. *Trans. China Electrotech. Soc.* **2020**, *35* (Suppl. S1), 172–181.